

## A RELIABLE METHOD FOR THE STABILITY ANALYSIS OF STRUCTURES

V. V. Galishnikova<sup>1\*</sup>, E. V. Lebed<sup>2</sup>

<sup>1</sup>Department of Architecture&Civil Engineering, RUDN University, Moscow, Russia

<sup>2</sup>Department of Structural Engineering, Moscow State University of Civil Engineering,  
Moscow, Russia

Published online: 24 November 2017

---

### ABSTRACT

A space truss is in an unstable configuration if it can displace incrementally without an incremental change in its loading and its supports. The load path which follows after an unstable configuration can be unique (snap-through), or there can be several possible load paths (bifurcation). This paper presents a method to detect nearly unstable configurations of a truss, a method to determine the loading, displacements and reactions of the unstable configuration and a method to traverse the load path which follows after the unstable configuration. The detection of structural configurations with singular tangent stiffness matrix is essential because they can be unstable. The secondary paths, especially in unstable buckling, can play the most important role in the loss of stability and collapse of the structure. A new method for reliable detection and accurate computation of singular points on load paths is presented and applied to a space truss subjected to symmetric and asymmetric snow loads.

**Keywords:** space structure, stability, snap-through, bifurcation, nonlinear behaviour.

---

Author Correspondence, e-mail: [galishni@yandex.ru](mailto:galishni@yandex.ru)

doi: <http://dx.doi.org/10.4314/jfas.v9i7s.45>



## 1. NONLINEAR STRUCTURAL ANALYSIS AND STABILITY ANALYSIS

Consider a structural model consisting of nodes, elastic finite elements, loads applied at nodes and displacements prescribed at nodes. The free displacements of the nodes in the direction of the applied loads and the reactions at the supports in the direction of the prescribed displacements are to be determined. The behaviour of the structure is described with a node displacement vector  $d$  and a node force vector  $f$ . The elements of  $d$  and  $f$  are ordered so that the free displacements precede the prescribed displacements. Vectors  $d$  and  $f$  are related by the total stiffness matrix  $K$  of the structure, which is decomposed into submatrices  $K_{im}$  that are compatible with the subdivision of  $d$  and  $f$ :

$$K d = f \quad (1)$$

$$\begin{matrix} K_{11} & K_{12} \\ K_{21} & K_{22} \end{matrix} \begin{matrix} d_1 \\ d_2 \end{matrix} = \begin{matrix} f_1 \\ f_2 \end{matrix} \quad (2)$$

$d_1$  – free displacements;  $d_2$  – prescribed displacements;  $f_1$  – applied loads;  $f_2$  – support reactions.

Consider a structure that is subjected to a load pattern and a displacement pattern so that the loading can be varied with a single parameter, which is called the load factor  $\lambda$ :

$$f_1 = \lambda f_{1p} \quad (3)$$

$f_{1p}$  - pattern load;

$$d_2 = \lambda d_{2p} \quad (4)$$

$d_{2p}$  - prescribed displacement pattern.

The behavior of the structure under load is described with a load path which shows the variation of the force norm with the displacement norm. Each point on the load path is an equilibrium configuration of the structure. If the displacements are large relative to the dimensions of the structure, the nonlinearity of the relationship between force norm and displacement norm must be considered as shown in Fig. 1.

The analysis of the load path of the structure consists of four parts: nonlinear analysis of the primary branch, determination of the singular point (if it exists for the specific structure and its loading), branch switching from the primary to the secondary branch and traversal of the secondary branch. This paper focuses on the reliable identification and accurate computation of singular points. Branch switching and continuation of load paths on secondary branches are

treated in [1], and were also presented in [2].

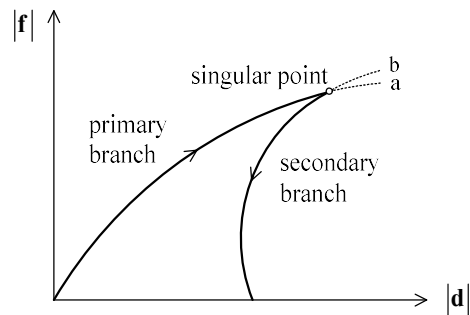


**Fig.1.** Nonlinear load path of a structure

It is essential to differentiate explicitly between a nonlinear analysis and a stability analysis of a structure. A nonlinear structural analysis starts with the reference configuration and computes the primary branch of the load path stepwise: It is therefore the solution of an initial value problem. The stability analysis also starts with the path following method at the origin. It goes beyond the nonlinear analysis by detecting and computing configurations (if they exist) in which the tangent stiffness matrix of the structure is singular. These configurations are mapped to the load path as singular points.

If the load factor decreases on one of the branches that leave a singular point, the structure is called unstable. The essential feature of a stability analysis is not only that it detects singular points, but also that it follows an unstable branch of the load path (if it exists) beyond the singular point. In Fig. 1, a nonlinear structural analysis may follow branch “a” beyond the singular point, whereas a stability analysis must follow the secondary branch. It will be shown later in this paper that it cannot be assumed that commercial software packages for nonlinear structural analysis automatically perform a stability analysis.

## 2. DETECTION OF SINGULAR POINTS

Path following methods that compute the primary branch of the load path in Fig. 1 are treated in detail in the literature, for example in monographs on nonlinear analysis of continua and structures by some publications[3-8]. The methods of analysis differ primarily in the type of the stiffness matrix (tangent, secant) and the control parameters for the step length (force, displacement, path length). Our work [5] has shown that a method based on iterative improvement of the secant stiffness matrix in each load step is particularly robust and

accurate. The governing equations for load step  $s$  are given by:

$$K_s^{(s)} Vd^{(s)} = Vf^{(s)} + c^{(s)}$$

$$\frac{K_{s11}}{K_{s21}} \frac{K_{s12}}{K_{s22}} \frac{\Delta d_1}{V\lambda d_{2p}} = \frac{V\lambda f_1}{Vf_2} + \frac{c_1}{c_2} \quad (5)$$

$K_s^{(s)}$  - secant stiffness matrix for step  $s$ ;  $Vd^{(s)}$  - displacement increment in step  $s$ ;  $Vf^{(s)}$  - force increment in step  $s$ ;  $c^{(s)}$  - unbalanced forces in state  $s$ .

The system stiffness is computed in the usual manner by adding the element contributions in global space. All nonlinear terms are retained in the formulation of the element stiffness matrices. Displacement derivatives that make the expressions for the stiffness coefficients nonlinear or unsymmetric are approximated numerically by their value in the preceding cycle of iteration in the load step, thus making the equations linear. The load factor increment is determined so that the arc lengths for the load steps on the load path have the same length. For the solution of governing equation in [1] the system matrix is decomposed into a diagonal matrix  $D$ , a left triangular matrix  $L$  with diagonal coefficients 1 and the transpose of  $L$ :

$$K_s^{(s)} = LDL^T \quad (6)$$

Since the product of the eigenvalues of stiffness matrix  $K$  equals the product of the diagonal coefficients of  $D$ , the diagonal coefficient of  $D$  with the smallest absolute value can be used to detect configurations of the structure that lie in the vicinity of singular points where at least one eigenvalue of  $K$  is null [5].

### 2.1. Example: Detection of a Singular Point

The detection of a singular point is illustrated for the spherical dome in Fig. 2 with spherical radius 29.0 m, base radius 19.5 m and height 7.531 m. All bars of the truss have an area of 0.002398 and a modulus of elasticity of 0.70e8 (units m, kN). The dome has rigid support contour and is subjected to the self weight of the bars and a sheet cover as well as symmetric and unsymmetrical snow loads according to the code of Russian Federation. The intensity of the symmetric snow load at the apex in load combination C1 is 1.57. The reference intensity of the eccentric snow load in load combination C2 is 1.80.

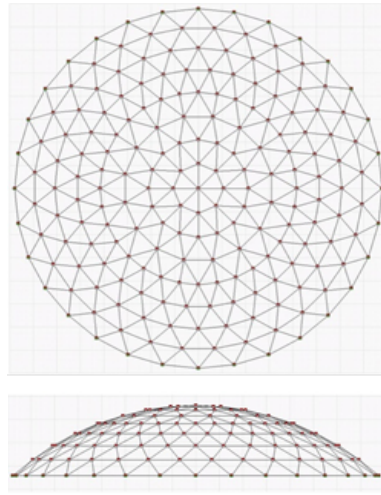


**Fig.2.** Plan and elevation of a spherical dome

Fig. 3 shows the variation of the smallest diagonal coefficient of  $D$  with the load factor for load combinations C1 and C2. The rate of decrease in the smallest diagonal coefficient increases significantly as the singular point is approached. The curves are nearly orthogonal to the load factor axis at the point of intersection. The smallest diagonal coefficient decreases more rapidly for the eccentric snow load in C2 than for the symmetric snow load in C1. The smallest diagonal coefficient in  $D$  is a suitable measure for vicinity of a dome configuration to a singular point.

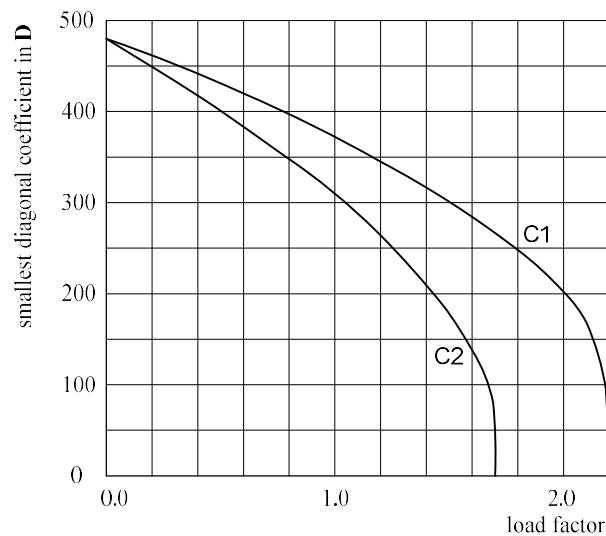


**Fig.3.** Smallest diagonal coefficient in the decomposition of the secant stiffness matrix

### 3. COMPUTATION OF A SINGULAR POINT

The load factor, displacement state and reaction state at a singular point are derived from the condition that the determinant of the tangent stiffness matrix is null at this point. The diagram in Fig. 3 cannot be used for this purpose, since it shows the diagonal coefficients for the secant stiffness matrix and none of the computed coefficients is exactly equal to null.

A structure is assumed to be in a nearly singular state if at least one of the coefficients of the diagonal matrix  $D$  in (6) changes sign in the next load step. Assume that a nearly singular state of the structure has been determined. Several methods are described in some literatures [4-7] which can be applied to step from a nearly singular point to a singular point.

In section 21.1 [4] describes bracketing procedures for the computation of singular points. He considers the determinant of the tangent stiffness matrix, the smallest coefficient in  $D$  and the smallest eigenvalue of the stiffness matrix as possible test functions for singular points. The chosen test function is computed at a point that lies before the singular point on the load path, and for a point that lies beyond the singular point. The test function is interpolated with the load factor or the arc length as control parameter. The value of the control parameter is determined for which the test function is null. The interpolated state is in general not an equilibrium state of the structure. The interval in which the singular point lies is reduced further by replacing one of the two test points by the interpolated point and repeating the procedure. Equilibrium at the interpolated points may have to be improved by iteration. The rate of convergence of the method is less than quadratic.

Wagner [7] formulates a direct method for the determination of singular points. He assumes that the algebraic governing equations of the finite element method for displacements  $v$  and load factor are given by

$$G(v, \lambda) = 0 \quad (7)$$

In section 8.1 of [6] this equation is expanded with the condition that the determinant of the tangent stiffness matrix must be null at a singular point. A further condition  $f$  is added to control the arc length in a load step:

$$\bar{G}(v, \lambda) = \begin{Bmatrix} G(v, \lambda) \\ f(v, \lambda) \\ \det K_t(v, \lambda) \end{Bmatrix} = 0 \quad (8)$$

The condition on the tangent matrix at the singular point is replaced by the special eigenvalue problem with eigenvalue null:

$$K_t \phi = \omega \phi \text{ with } \omega = 0 \quad (9)$$

In section 8.4 of [6] the following governing equations are derived from (8) and (9) by means of consistent linearization:

$$\begin{bmatrix} K_t & -P & 0 \\ (K_t \phi)_{,v} & (K_t \phi)_{,\lambda} & K_t \\ 0^T & 0 & P^T \end{bmatrix} \begin{bmatrix} V_v \\ V_\lambda \\ V_\phi \end{bmatrix} = \begin{bmatrix} 0 \\ 0 \\ 0 \end{bmatrix} \quad (10)$$

$P$  - pattern load vector.

The solution of equation (10) yields an approximation for the step from a nearly singular to the singular point. The solution is an approximation because the tangent stiffness matrix is computed at the nearly singular point. The method requires the determination of the derivatives in the second row of (10). The system of equations is not symmetric, but can be solved effectively with a special technique described in section 8.3 of [6].

The authors have developed a new method for the computation of singular points which follows an entirely different concept than the methods proposed by Crisfield [4] and Wagner [7]. The method expresses the tangent stiffness matrix at the singular point in terms of the displacement increment and the unknown load factor increment for the step from the nearly singular point to the singular point. The load factor increment is found to be the eigenvalue of the resulting general eigenvalue problem. The method is formulated in the following paragraphs.

Assume that the unbalanced forces at the nearly singular point are reduced by iteration so that they can be neglected in equation (5). The resulting equations are solved for the displacement increment in the step from the nearly singular to the singular point:

$$Vd = V\lambda \frac{d_{1c}}{d_{2p}} \quad \text{with } d_k = K_{s11}^{-1} (f_{1p} - K_{s12} d_{2p}) \quad (11)$$

The displacement increments (11) are used to compute the displacement state at the singular point, retaining the load factor increment as unknown. These displacements are then used to express the tangent stiffness matrix at the singular point in terms of the unknown load factor increment. The determinant of the tangent stiffness matrix is set to null:

$$\det K_{11c} = \det(K_0 + V \lambda K_1) = 0 \tag{12}$$

$K_{11c}$  submatrix  $K_{11}$  of tangent stiffness matrix at the singular point.

Condition (12) is satisfied by solving the associated general eigenvalue problem. The eigenstate in (13) with the smallest absolute eigenvalue determines the singular point.

$$K_0 \phi = -V \lambda K_1 \phi \tag{13}$$

The matrices in (13) are derived for space trusses with bar elements in [2]. The element displacement increment is derived from the system displacement increment:

$$V v_o = R_o^T T_o V d \tag{14}$$

$V v_o$  - increment of the element displacement vector in element reference space;

$R_o$  - element rotation matrix from global space to element reference space;

$T_o$  - element topology matrix.

Consider a point on the axis of the bar. The displacement is interpolated linearly over the length of the bar. The derivatives of the coordinates of the displacement increments at the point with respect to the axial coordinate are:

$$V v_{m,1} = V \lambda d_m \tag{15}$$

with  $d_m = \frac{1}{a} g_m^T R_e^T T_e d_{1c}$  and  $m \in \{1, 2, 3\}$

$$g_1^T = \begin{bmatrix} -1 & 0 & 0 & 1 & 0 & 0 \end{bmatrix}$$

$$g_2^T = \begin{bmatrix} 0 & -1 & 0 & 0 & 1 & 0 \end{bmatrix}$$

$$g_3^T = \begin{bmatrix} 0 & 0 & -1 & 0 & 0 & 1 \end{bmatrix}$$

$a$  - length of the bar.

The derivatives  $\bar{v}_{m,1}$  of the displacement coordinates at the singular point are thus:

$$\bar{V}_{m,1} = V_{m,1} + V \lambda d_m \tag{16}$$

$V_{m,1}$  - displacement derivative at the nearly singular point

The vector products of the derivative vectors are denoted as follows:

$$G_{kk} := g_k g_k^T \quad G_{km} := g_k g_m^T + g_m g_k^T \tag{17}$$

$$k, m \in \{1, 2, 3\}$$

The tangent stiffness matrix for a bar with area  $A$  and modulus of elasticity  $E$  is shown in [2]:

$$K_e = K_c + K_g + K_d \quad (18)$$

$$K_c = \frac{AE}{a} G_{11} \quad K_c = \frac{AE}{a} c_0 (G_{11} + G_{22} + G_{33}) \quad (19)$$

$$C_0 = \bar{V}_{1,1} + \frac{1}{2} (\bar{V}_{1,1}^2 + \bar{V}_{2,1}^2 + \bar{V}_{3,1}^2)$$

$$K_d = \frac{AE}{a} (c_2 G_{11} + c_3 G_{22} + c_4 G_{33} + c_5 G_{12} + c_6 G_{13} + c_7 G_{23}) \quad (20)$$

$$c_2 = \bar{V}_{1,1} (2 + \bar{V}_{1,1}); \quad c_3 = \bar{V}_{2,1}^2; \quad c_4 = \bar{V}_{2,1}^2;$$

$$c_5 = \bar{V}_{2,1} (1 + \bar{V}_{1,1}); \quad c_6 = \bar{V}_{3,1} (1 + \bar{V}_{1,1}); \quad c_7 = \bar{V}_{2,1} \bar{V}_{3,1}$$

Expression (16) is substituted into (19) and (20) to yield an element tangent stiffness matrix which is a quadratic function of the unknown load factor increment. The element matrices are assembled in the conventional manner to yield the system tangent stiffness matrix, which is also a quadratic function of the load factor increment:

$$K_t = K_0 + V \lambda K_a + V \lambda^2 K_b \quad (21)$$

The eigenvalue problem (13) is solved in two steps. In the first step, the last term in (21) is neglected so that (13) is solved for the second step, the load factor increment computed in the first cycle is used to solve (13) with (21). The second step is repeated if the change in the load factor increment is not sufficiently small.

The state which is determined with the general eigenvalue problem (13) is not an exact singular point because expression (11) for the displacement increment is a linear approximation. The computed state can be treated as an improved nearly singular state for which the procedure to determine the singular point is repeated. Numerical experience shows that a single repetition leads to a singular state that is highly accurate.

### 3.1. Example: Computation of Singular Points

The method described in section 4 has been applied to compute the singular points of the dome in Fig. 2 for load combinations C1 and C2. The states of the dome near the singular points are:

$$\text{C1: state 42: } \quad \lambda = 2.101 \ 688$$

state 43:	$\lambda = 2.201\ 795$	nearly singular point
state 44:	$\lambda = 2.193\ 810$	improved singular point
state 45:	$\lambda = 2.193\ 861$	singular point
C2: state 27:	$\lambda = 1.599\ 633$	
state 28:	$\lambda = 1.741\ 718$	nearly singular point
state 29:	$\lambda = 1.693\ 634$	improved singular point
state 30:	$\lambda = 1.693\ 639$	singular point

The eigenvector for the singular state of the dome for the symmetric snow load C1 is perfectly symmetric. This is illustrated in Fig. 4 with the vertical components of the normalized eigenvector corresponding to eigenvalue null. Ring 1 lies next to the apex of the dome.

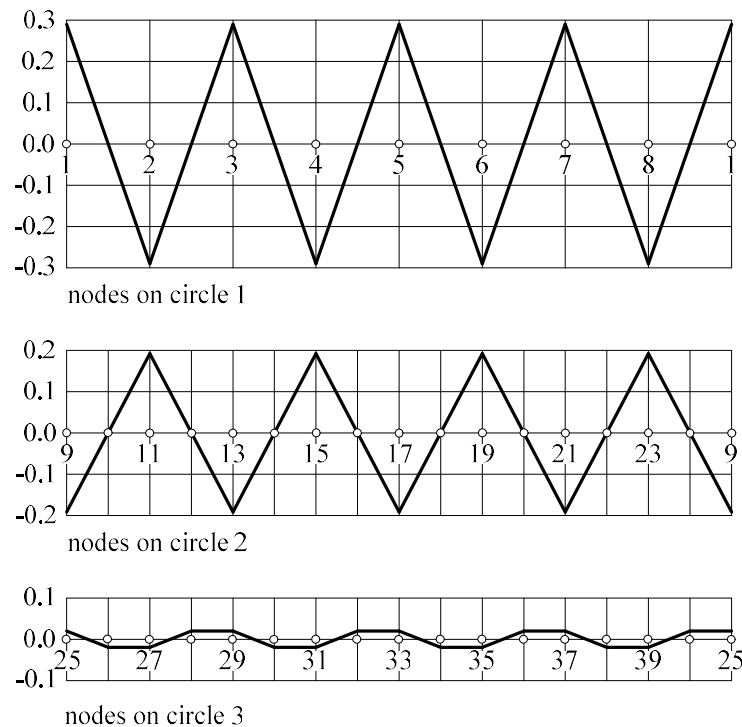


**Fig.4.** Vertical displacements in the normalized eigenvector for the singular state of C1

The computation of a singular point does not indicate whether the dome is unstable. In order to investigate the stability, the load path must be continued on the secondary branch. This topic is treated in [1]. It is shown that both load combinations have unstable singular points. The continuation also leads to the buckled shape of the dome.

The buckling zone for C1 is centered at the apex. The displacements of neighboring nodes on ring 1 are shown in Fig. 5 and Fig. 6. The load factor reaches a maximum value at the singular

point. For one node, the displacements continue to increase on the secondary branch, whereas they decrease for the other node. This corresponds to the eigenvector in Fig. 4.

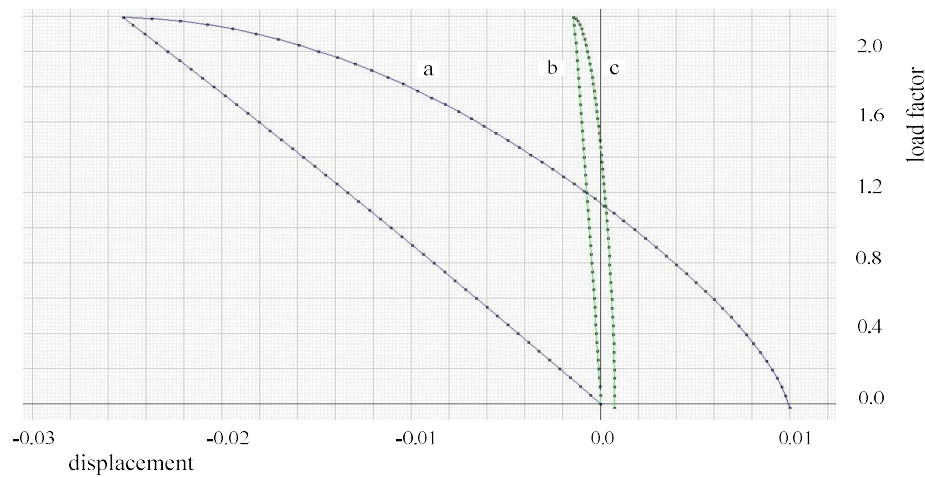


**Fig.5.** Variation of load factor with displacement at node n2 on ring 1 for C1  
(a) vertical displacement component; (b) and (c) horizontal displacement components

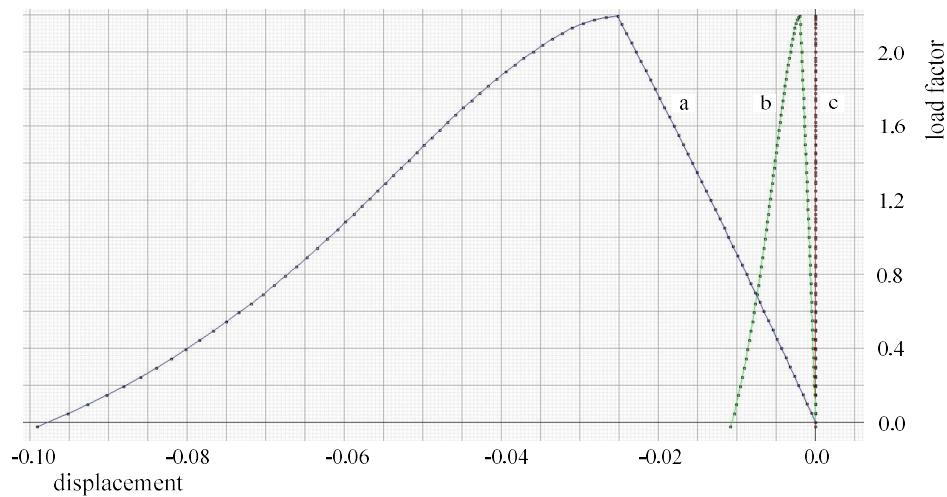


**Fig.6.** Variation of load factor with displacement at node n3 on ring 1 for C1  
(a) vertical displacement component; (b) and (c) horizontal displacement components

The buckling zone for C2 is eccentric in the direction of the snow load eccentricity. The extent of the buckling is local. It is centered on the fourth ring from the apex. The displacements of two nodes in the buckled zone is shown in [1]. As for C1, the displacements for one node increase on the secondary path, whereas those of the neighboring node decrease. The load paths of the dome for load combinations C1 and C2 are shown in (11). The load paths almost reverse onto themselves at the singular points.

#### 4. CONCLUSION

The oil tank cap has been designed with significant resistance against buckling. The buckling zone for symmetric snow load is symmetric. It is close to the apex of the dome.

The cap subjected to distributed load does not displace significantly prior to buckling. The displacement history is essentially linear. When the dome buckles, alternate nodes in ring 2 displace into and out of the volume of the dome. The stationary point is a bifurcation point.

The buckling zone for eccentric snow load lies in the half of the cap that carries the eccentric snow load and is centred on the axis of symmetry of the load. It is midway between the apex and the supports of the dome. As in the case of symmetric snow load, the dome does not displace significantly prior to buckling. Its displacement history is nearly linear. The stationary point is a snap-through point.

The example confirms that the new theories and numerical methods described in the paper can be regarded as an advance in the stability analysis of slender structures for civil engineering practice.

#### 5. ACKNOWLEDGEMENTS

This research work was financially supported by the Ministry of Education & Science of the Russian Federation (Agreement No. 02.A03.21.0008).

#### 6. REFERENCES

- [1] Galishnikova V.V. A New Expansion Method for Continuation of Load Paths at Singular Points. *Journal of People Friendship University of Russia: Mathematics, Informatics and Physics*, 2011, 2: 104-113.
- [2] Galishnikova V.V. Analytical Solution of the Nonlinear Stability Problem of a 3D Truss. *Journal of Volgograd State University for Architecture and Civil Engineering: Natural Science*, 2007, 6(23): 53-64.
- [3] Belytschko T., Liu W. and Moran B. *Nonlinear Finite Elements for Continua and Structures*. John Wiley & Sons, New York, USA, 2000.
- [4] Crisfield M.A. *Nonlinear Finite Element Analysis of Solids and Structures: Vol. 1*. John Wiley & Sons, New York, USA, 1997.

- 
- [5] Galishnikova V., Dunaiski P. and Pahl P.J. Geometrically Nonlinear Analysis of Plane Trusses and Frames. Sun Press, Stellenbosch, Germany, 2009.
- [6] Reddy J.N. An Introduction to Nonlinear Finite Element Analysis. Oxford University Press, Oxford, UK, 2004.
- [7] Wagner W. Zur Behandlung von Stabilitätsproblemen der Elastostatik mit der Methode der Finiten Elemente. Bericht Nr. F91/1, Bereich Mechanik der Universität Hannover, Germany 1991.
- [8] Wriggers P. Nichtlineare Finite-Element-Methoden. Springer Verlag, Germany, 2001.

**How to cite this article:**

Galishnikova V V, Lebed E V. A reliable method for the stability analysis of structures. *J. Fundam. Appl. Sci.*, 2017, *9(7S)*, 484-496.